Organic Electronics 31 (2016) 234–239

Contents lists available at ScienceDirect

Organic Electronics

journal homepage: www.elsevier.com/locate/orgel

Realizing improved performance of down-conversion white organic light-emitting diodes by localized surface plasmon resonance effect of Ag nanoparticles

Jinbo Hu [a, b, 1], Yue Yu [b, 1], Bo Jiao [b, **], Shuya Ning [c], Hua Dong [b], Xun Hou [b], Zhengjun Zhang [a], Zhaoxin Wu [b, *]

[a] School of Physics, Northwestern University, Xi'an, 710069, China
[b] Key Laboratory for Physical Electronics and Devices of the Ministry of Education & Shanxi Key Lab of Information Photonic Technique, School of Electronic and Information Engineering, Xi'an Jiaotong University, Xi'an, 710049, China
[c] College of Science, Shaanxi University of Science and Technology, Xi'an, 710021, China

ARTICLE INFO

Article history:
Received 24 November 2015
Received in revised form
21 January 2016
Accepted 21 January 2016
Available online 3 February 2016

Keywords:
White organic light-emitting diodes
Down-conversion
Localized surface plasmon resonance
Ag nanoparticles

ABSTRACT

Down-conversion structure white organic light-emitting diodes (WOLEDs), in which white light is generated by a blue emission organic light-emitting diodes (OLEDs) in combination with a color conversion layer (CCL) outside the substrate, has attracted extensive interest due to its significant advantages in low cost and stabilized white-light emissions. However, low color-conversion efficiency of CCL is still a bottleneck for the performance improvement of down-conversion WOLEDs. Here, we demonstrate an approach to enhance the color-conversion efficiency of CCL-WOLEDs by localized surface plasmon resonance (LSPR) effect. In this approach, a blend of Ag nanoparticles and polyvinyl alcohol (PVA) is solution-deposited between the blue organic light emitting diodes and color-conversion layer. Based on the LSPR effect of this modified structure, the color conversion efficiency has improved 32%, from 45.4% to 60%, resulting a 14.4% enhancement of the current efficiency, from 9.73 cd/A to 11.14 cd/A. Our work provides a simple and low-cost way to enhance the performance of down-conversion WOLEDs, which highlights its potential in illumination applications.

1. Introduction

White organic light-emitting diodes (WOLEDs) have drawn significant interest due to its remarkable advantages, such as surface lighting source, high color rendering capability, low cost, and easy for flexible devices [1–3]. Generally, the WOLEDs can be obtained by four approaches [4,5]: 1) single emissive layer doped with red, green, and blue (RGB) emissive components [6–8], 2) vertical stacking of RGB emission structures [9], 3) horizontal stacking of RGB emission units [4], 4) down-conversion structure generated by a complementary color conversion layer (CCL) in combination with a single blue emission organic light-emitting diodes (OLED) [10–12]. Among these approaches, the down-conversion structure exhibits great potential in illumination application due to its low cost fabrication and excellent color stability under different driven voltage. In order to improve the performance of down-conversion WOLEDs, some research works have been reported [13]. In addition to enhance the light outcoupling of blue OLED unit, improving converting ability of CCL becomes a vital issue. Yu-Hsuan Ho et al. introduced periodical nanospheres between the blue OLED and the red phosphor, increased the effective light path to achieve high-efficiency color conversion [4,10,13–15]. Benjamin C. and co-workers reported the extraordinary enhancement of the device's external light output due to the better phosphor layer based on a nitridosilicate phosphor ($[Sr,Ba,Ca]_2Si_5N_8:Eu^{2+}$) in CCL [4].

Localized surface plasmons (LSPs) are charge density oscillations confined to metallic nanoparticles, and the excitation of LSPs by an electric field at an incident wavelength where resonance occurs results in an enhancement of the local electromagnetic fields [16–21]. Localized surface plasmons resonance (LSPR) effect has aroused considerable attention in fluorescent enhancement [22], high-efficiency organic solar cells and simple monochromatic

* Corresponding author.
** Corresponding author.
E-mail address: zhaoxinwu@mail.xjtu.edu.cn (Z. Wu).
[1] These authors contributed equally to this work.

http://dx.doi.org/10.1016/j.orgel.2016.01.031
1566-1199/

OLEDs [16,17,23]. In this work, a performance enhancement of down-conversion WOLED is first demonstrated based on the LSPR effect of Ag nanopaticles (Ag Nps). We chose the high efficient material iridium (III) [bis(4,6-difluoropheny)-pyridinato-N,C2'] picolinate (Firpic) as a blue-emitter layer in blue OLED unit, and a fluorescent dye poly(2-methoxy-5-(2-ethyl-hexyloxy)-1,4-phenylene-vinylene) (MEHPPV) as a CCL. By inserting the Ag Nps layer into substrate/CCL interface, the color conversion efficiency has improved 32%, from 45.4% to 60%, resulting a 14.5% enhancement of the current efficiency, from 9.73 cd/A to 11.14 cd/A.

2. Experimental methods

2.1. Fabrication and characterization of the color-conversion layer with Ag Nps

Ag Nps used in this study were synthesized according to the report of Subrata Kundu [24–27]. As shown in Fig. 1(a), the size of Ag Nps distributed around 80 nm. To reduce the agglomeration of Ag Nps, the Ag Nps aqueous solution was mixed uniformly with 40 mg/ml polyvinyl alcohol (PVA) at the volume ratio of 1:1. Indium tin oxide (ITO) glass with a sheet resistance of 25Ω/□ was used as substrate. After being cleaned with deionized water and organic solvents and exposed into an UV-ozone atmosphere, the mixed solution of Ag Nps and PVA was spin-coated at 1000 rpm for 30 s onto the glass side of indium tin oxide (ITO) substrate to form the film with Ag Nps. Then the film was thermally annealed at 140 °C under atmosphere for 20 min. The Ag Nps film was characterized by atomic force microscope (AFM). Ag Nps distributed evenly on the glass surface with no significant agglomeration, as shown in Fig. 1(b). After cooling down of Ag Nps film, MEHPPV solution with concentration of 6 mg/ml was spin-coated at 3000 rpm for 30 s on the Ag Nps film and annealed at 80 °C for 5 min. The thickness of MEHPPV film was around 60 nm.

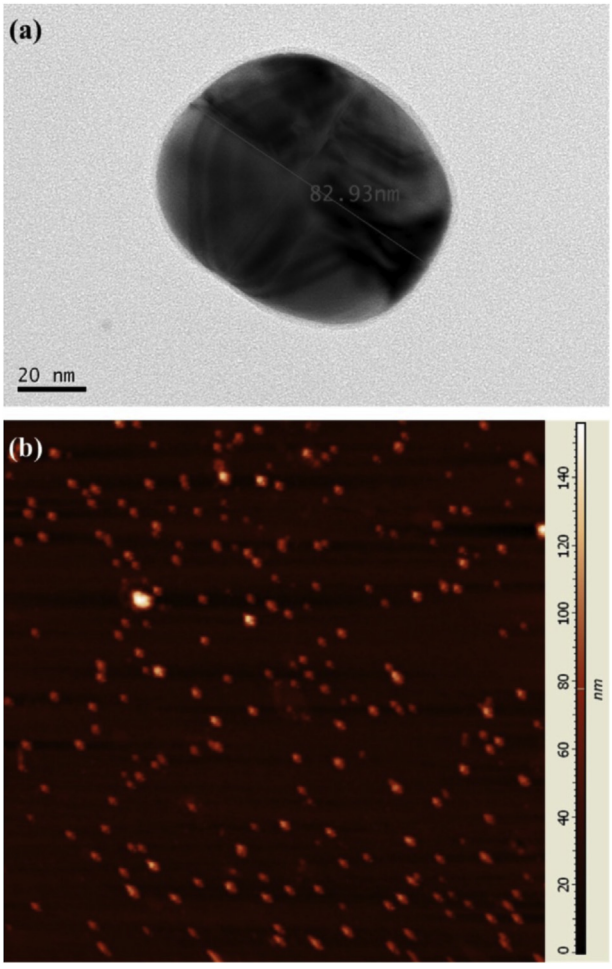

Fig. 1. (a) TEM images of Ag Nps; (b) AFM image of Ag-PVA thin film.

2.2. OLED fabrication and characterizations

OLEDs were fabricated onto a cleaned glass substrate by thermal evaporation at a pressure of 1×10^{-3} Pa without vacuum break. The thickness of the films was determined using a quartz-crystal sensor. Emission area of the device was about 12 mm^2. The voltage–current density (V–J) and voltage–brightness (V–L) characteristics of the devices were measured with a Keithley 2602 source meter. All the measurements were carried out at room temperature under ambient conditions. Photoluminescence (PL) and absorption spectra were recorded by a Horiba Jobin Yvon Fluoromax-4 spectrophotometer and a Hitachi UV 3010 spectrophotometer, respectively. The PR650 spectrophotometer and fiber optic spectrometer were utilized to measure the electroluminescent (EL) spectra. Four different devices were fabricated and tested. As shown in Fig. 2, the configuration details of these devices are shown as below:

Device 1: MEHPPV (60 nm)/PVA (60 nm)@Ag Nps/Glass/ITO/HATCN (10 nm)/TAPC (45 nm)/Mcp: Firpic 10 wt% (20 nm)/Tmpypb (45 nm)/LiF (1 nm)/Al.

Device 2: MEHPPV (60 nm)/PVA (60 nm)/Glass/ITO/HATCN (10 nm)/TAPC (45 nm)/Mcp: Firpic 10 wt% (20 nm)/Tmpypb (45 nm)/LiF (1 nm)/Al.

Device 3: PVA (60 nm)@Ag Nps/Glass/ITO/HATCN (10 nm)/TAPC (45 nm)/Mcp: Firpic 10 wt% (20 nm)/Tmpypb(45 nm)/LiF (1 nm)/Al.

Device 4: PVA (60 nm)/Glass/ITO/HATCN (10 nm)/TAPC (45 nm)/Mcp: Firpic 10 wt% (20 nm)/Tmpypb (45 nm)/LiF (1 nm)/Al.

Device 1 is white device with PVA@Ag Nps and Device 2 is the control device, Device 3 is blue device with PVA@ Ag Nps Ag and Device 4 is also fabricated for comparison. Here di-[4-(N,N-ditolyl-amino)-phenyl]cyclohexane (TAPC) and 1,3,5-tri[(3-pyridyl)-phen-3-yl]benzene (Tmpypb) were used as the hole-transport layer and

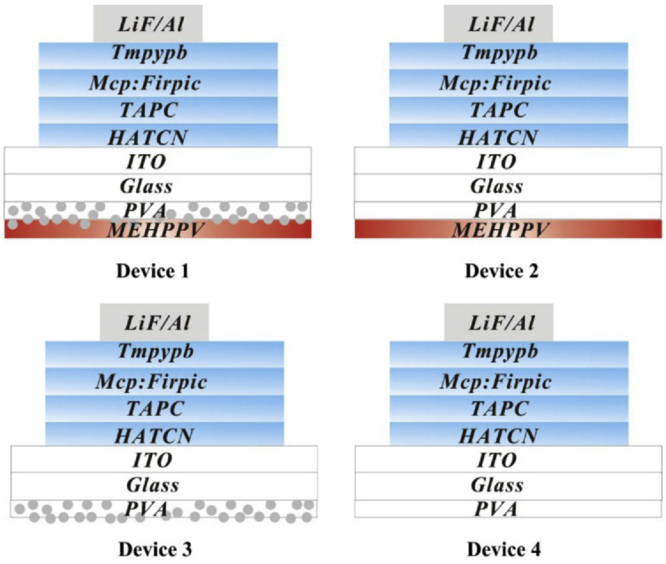

Fig. 2. Schematic structures of the Device 1, Device 2, Device 3 and Device 4 respectively.

electron-transport layer respectively due to their high carrier transport and exciton confinement capabilities. The optimal doping ratio for 3-bis(9-carbazolyl)benzene (Mcp):Firpic was 10 wt%.

3. Results and discussions

As shown in Fig. 3(a), the color conversion material exhibits strong absorption from 450 nm to 550 nm and emission with the peak wavelength at 590 nm. The electroluminescence peak of the blue device is approximate 472 nm, which has a high overlap efficiency with the absorption spectrum of MEHPPV, so the energy transfer is efficient from emitting layer in blue OLED to the CCL. The UV–vis absorption spectra of the Ag Nps displayed a surface plasmon absorption from 390 nm to 550 nm with band centered at 450 nm, which echoes the report by Park's report very well [23]. It is considered that LSPR will be excited easily because the emission of Firpic quite agrees with the absorption of Ag Nps. As shown in Fig. 2(b), when the Ag Nps and PVA blend film is inserted into Glass/MEHPPV interface, PL intensity enhancement of 1.8 times can be observed compared with the control film without Ag Nps.

Typically, fluorescence enhancement of LSPR effect can be understood in two different mechanisms. one is the significant optical absorption enhancement. Once incident spectra and UV–vis absorption spectra of Nps overlap well, strong local plasmons field around metal Nps will be generating. Optical absorption of fluorescence molecules is enhanced when molecules are placed near metal Nps, the absorption coefficient of the fluorescent molecules depend on the local plasmons field intensity. Under the intense electric field, the population of the excited state fluorescent will increase. On the other hand, emission intensity can be enhanced by LSPs coupling with exciton emission or fluorescence molecule excitation. This situation would occur on condition that there is an overlap between emitting spectra of fluorescence molecule and UV–vis absorption spectra of metal Nps. LSPR-exciton coupling process is much faster than spontaneous recombination of excitons, so we obtain reduced decay time of fluorescence molecule PL. For the lack of spectra overlap between UV–vis absorption spectra of Ag Nps and PL spectra of MEHPPV in our work, PL enhancement mechanism mainly belongs to the first one.

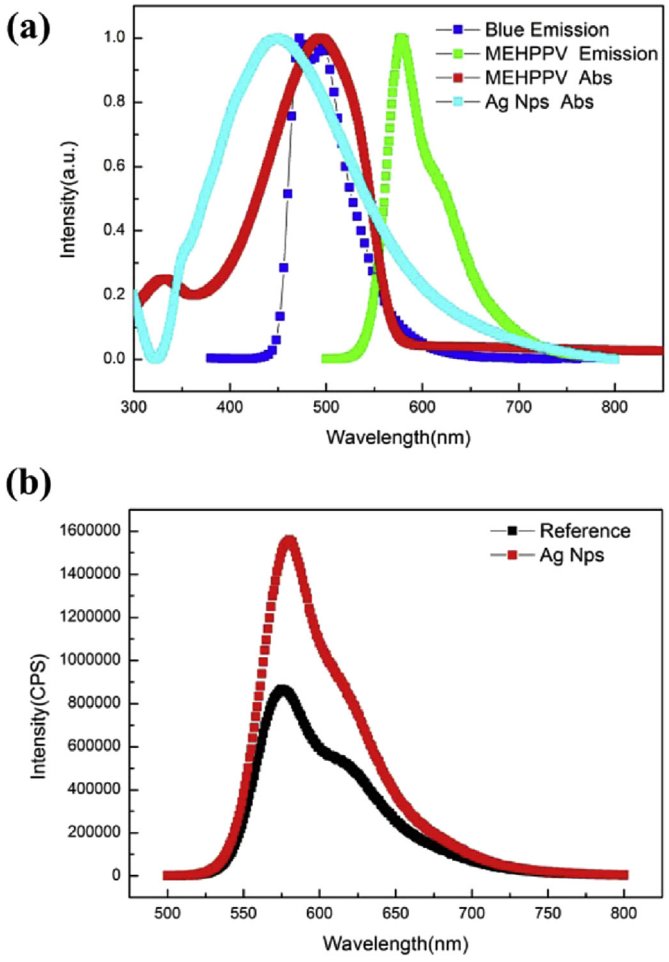

Fig. 3. (a) Absorption and PL spectra of the emitters as well as absorption of Ag Nps; (b) Emission spectra of sample with/without Ag Nps excited wavelength is localized at 472 nm.

Fig. 4(a) exhibits the current–voltage–luminance–efficiency (I–V–L–η) characteristics of these devices, current–voltage curves of Device 1, 2, 3 and 4 are almost the same, which means the fabrication process of Ag Nps layer dose not influence the electronic property of these devices. As shown in Fig. 4(b), for white Device 1 and 2, the peak current efficiency are 11.14 cd/A and 9.73 cd/A, and the peak luminance are 9361 cd/m^2 and 6331 cd/m^2, respectively. The white Device 1 with Ag Nps exhibited a nearly 14.5% improvement of efficiency compared to Device 2 due to the LSPR effect of the Ag Nps. To investigate the influence of the Ag Nps on the Devices, Device 3 and Device 4 were fabricated. The peak current efficiency of Device 3 and Device 4 are 28.25 cd/A and 29.9 cd/A, and the peak luminance were 22825 cd/m^2 and 30675 cd/m^2, respectively. There is a 5.8% efficiency loss for Device 3 compared to Device 4. The main reason for this phenomenon is that the Ag Nps could absorb the light from blue OLED unit.

Fig. 5(a) shows the normalized EL spectra for Device 1 and Device 2. There are three peaks, the left two peaks generated from the blue OLED unit, and the right peak generated from dye MEHPPV in the CCL. When CCL is incorporated with blue OLED, some blue emission of Firpic is absorbed and then converted to red fluorescence of MEHPPV resulting in a mixture of white emission. The red part of MEHPPV emission in the device with Ag Nps is obviously enhanced in comparison with the device without Ag Nps. This result suggests that the fluorescence of MEHPPV is enhanced by the LSPR effect around Ag Nps. The inset is the EL spectra, which is used to calculate the color conversion efficiency. As shown in Fig. 5(b), the inset EL spectra of Device 3 showed lower intensity compared with that of Device 4 because Ag Nps absorbed the light from blue unit, which matched well with the current efficiency.

Color conversion efficiency (CCE) is an important index to measure the conversion ability of CCL. The color conversion efficiency can be expressed as

$$color\ conversion\ efficiency = \frac{generation\ of\ red\ photons}{decrease\ of\ blue\ photos} \quad (1)$$

To study the conversion efficiency from blue light to red light, we divided the white emission spectra by Gaussian functions to calculate the photon densities for red and blue light. The color conversion ratio is defined as the photon density of converted red light divided by the decrease of blue light. The decrease of blue light is calculated by comparing the difference between blue OLEDs with and without the CCL.

$$color\ conversion\ efficiency = \frac{\eta_{c1}\cdot B_0}{\eta_{ext0}\cdot B_0 - \eta_{ext1}\cdot B_0}(Device\ 1)$$

$$= \frac{\eta_{c2}\cdot B_0}{\eta_{ext0'}\cdot B_0 - \eta_{ext2}\cdot B_0}(Device\ 2) \quad (2)$$

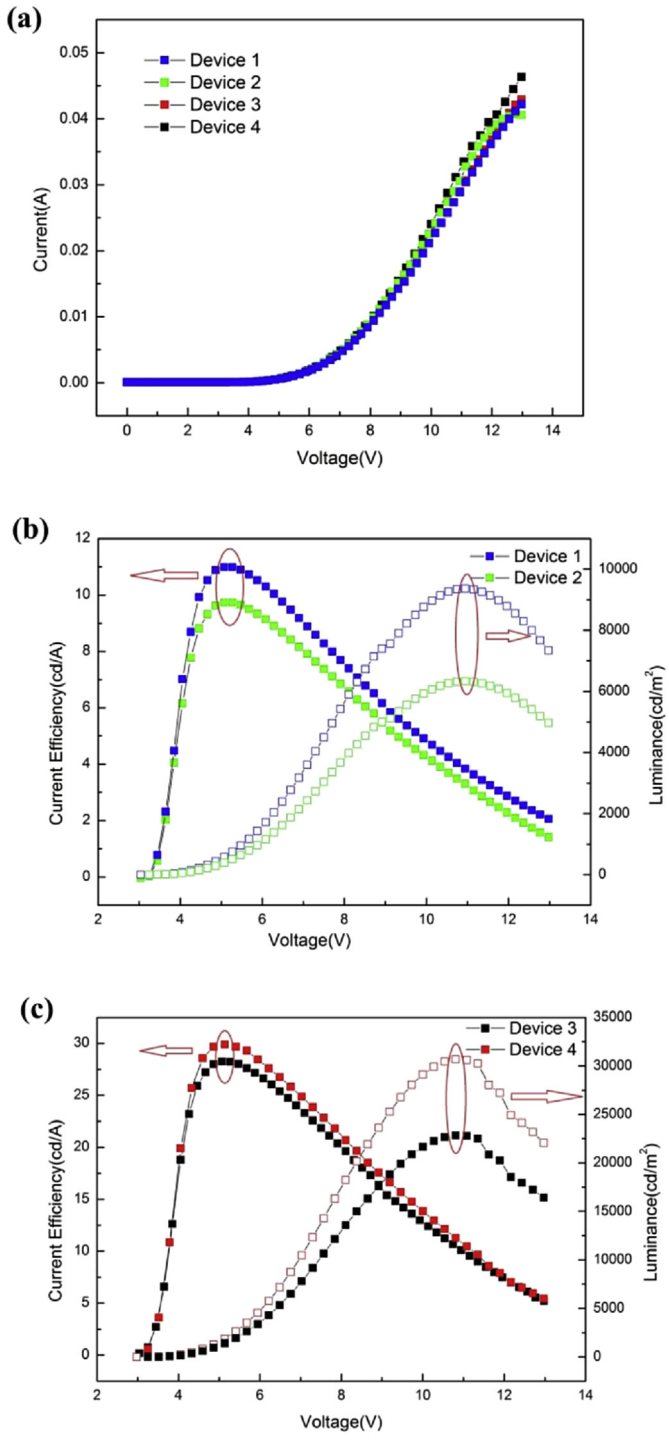

Fig. 4. (a) Current–voltage characteristics of the Device 1, Device 2, Device 3 and Device 4 respectively; (b) Current efficiency-Voltage-Luminance of the Device 1, Device 2 respectively; (c) Current efficiency-Voltage-Luminance of the Device 3 and Device 4 respectively.

As shown in Fig. 6, whereB_0 is the blue light photons density generated and η_{ext1}, η_{ext2}, η_{ext0}, $\eta_{ext0'}$ show the blue light photons extraction efficiency of the Device 1, Device 2, Device 3 and Device 4, respectively. Due to absorption of blue light by Ag Nps, η_{ext0} is slightly less than $\eta_{ext0'}$. As the same, η_{ext1} is slightly less than η_{ext2}. Due to the LSPR effect of Ag Nps, η_{c1} is more larger than η_{c2}, thus, the conversion ratio of Device 1 is greater than that of Device 2. Calculating from the CCE formula (2), the CCE of Device 1 and 2 are

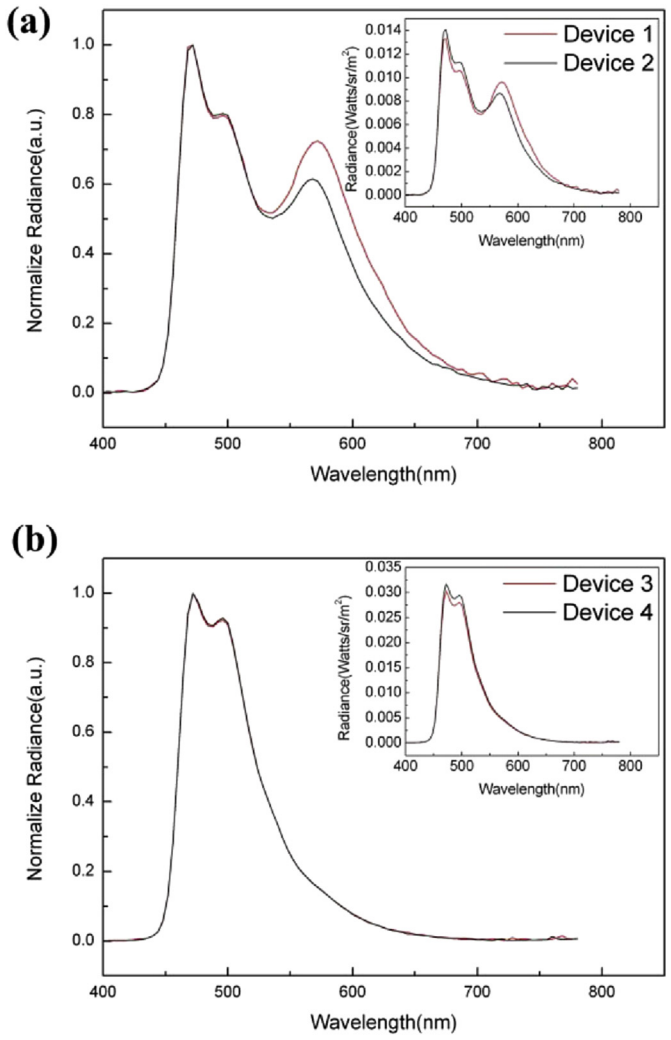

Fig. 5. (a) Normalized EL spectra for Device 1 and 2 at 5 V respectively; (b) Normalized EL spectra for Device 3 and 4 at 5 v respectively; Insets are non-normalized EL spectra.

60% and 45.4%, respectively. Compared to Device 2, there is a 32% enhancement for Device 1, therefore, Ag Nps act as an effective method in enhancing CCE of CCL.

It is well known that LSPR intensity decays almost exponentially with distance away from the nanoparticle surface [28]. Typically, 10-fold enhancement in the field intensity can be obtained at the Ag Np surface, and the decay constant is on the order of 10 nm. In order to verify the enhanced range of LSPR on the performance of CCL-WOLEDs, Device 5 and Device 6 with increased thickness of MEHPPV were fabricated. The configuration details are shown as below:

Device 5: MEHPPV (80 nm)/PVA (60 nm)@Ag Nps/Glass/ITO/HATCN (10 nm)/TAPC (45 nm)/Mcp:Firpic 10 wt% (20 nm)/Tmpypb (45 nm)/LiF (1 nm)/Al.

Device 6:MEHPPV (80 nm)/PVA (60 nm)/Glass/ITO/HATCN (10 nm)/TAPC (45 nm)/Mcp:Firpic 10 wt% (20 nm)/Tmpypb (45 nm)/LiF (1 nm)/Al.

Increased thickness of MEHPPV film leads to increased distance from MEHPPV molecules to Ag Nps, once the distance exceeds the effective range, LSP field strength will reduce to very low. Thus, increasing the thickness of MEHPPV reduces the fluorescence enhancement effect of Ag Nps, as shown in Fig. 7.

Furthermore, Fig. 8 shows the angular dependence of the emission for Device 1 and Device 2 as well as the ideal Lambertain

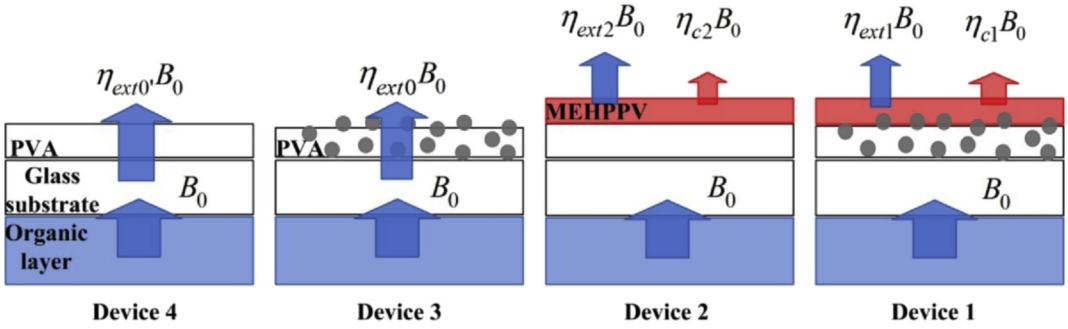

Fig. 6. Illustrations for parameters that used in color conversion efficiency calculation. (For interpretation of the references to colour in this figure legend, the reader is referred to the web version of this article.)

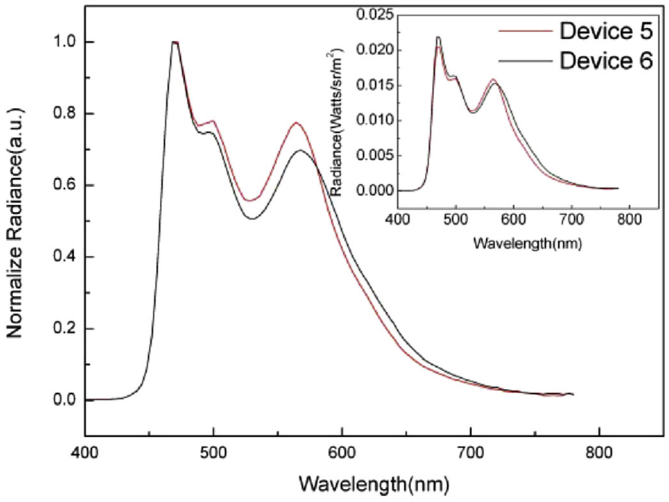

Fig. 7. Normalized EL spectra for Device 5 and 6 at 5 v respectively; the inset is the non-normalized EL spectra.

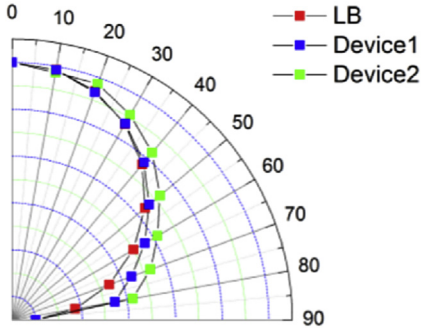

Fig. 8. Polar-plots of Devices 1 and 2 respectively.

curve for comparison. Device 1 exhibits a nearly Lambertian emission pattern, indicating that the Ag Nps CCL-based WOLEDs possess great potential for applications. This phenomena can be understood by the scattering effect because of the random nanostructure scattering layer, which not only inhibits the microcavity effect but also increases the effective light path and extracts the light limited in the device, thus closer to the Lambertain emitting [29,30].

4. Conclusions

In conclusion, we demonstrated LSPR–enhanced color conversion efficiency of down-conversion structure WOLED by introducing Ag Nps. The normalized EL spectra showed that LSPR of Ag Nps enhanced the red emission and color conversion efficiency in CCL. Based on the LSPR effect of this modified structure, the color conversion efficiency has improved 32%, from 45.4% to 60%, resulting a 14.5% enhancement of the current efficiency, from 9.73 cd/A to 11.14 cd/A. These results indicate that CCL combined with Ag Nps possesses great potential for use in display and lighting applications.

Acknowledgments

This work was financially supported by Basic Research Program of China (2013CB328705), National Natural Science Foundation of China (Grant Nos. 11574248;61275034;61106123), Ph.D. Programs Foundation of Ministry of Education of China (Grant No. 20130201110065). International Cooperation by Shaanxi (Grant No.2015 KW-008). The TEM work was done at International Center for Dielectric Research (ICDR), Xi'an Jiaotong University, Xi'an, China.

References

[1] Y. Shao, Y. Yang, White organic light-emitting diodes prepared by a fused organic solid solution method, Appl. Phys. Lett. 86 (2005) 073510–073513, 073510.
[2] J. Huang, G. Li, E. Wu, Q. Xu, Y. Yang, Achieving high-efficiency polymer white-light-emitting devices, Adv. Mater. 18 (2006) 114–117.
[3] B. Ma, P.I. Djurovich, S. Garon, B. Alleyne, M.E. Thompson, Platinum binuclear complexes as phosphorescent dopants for monochromatic and white organic light-emitting diodes, Adv. Funct. Mater. 16 (2006) 2438–2446.
[4] B.C. Krummacher, V.-E. Choong, M.K. Mathai, S.A. Choulis, F. So, F. Jermann, T. Fiedler, M. Zachau, Highly efficient white organic light-emitting diode, Appl. Phys. Lett. 88 (2006) 113506.
[5] K. Guo, B. Wei, Three-peak standard white organic light-emitting devices for solid-state lighting, International Symposium on Optoelectronic Technology and Application 20142014, pp. 929516–929516-929516.
[6] Y.W. Ko, C.H. Chung, H.L. Jin, Y.H. Kim, C.Y. Sohn, B.C. Kim, C.S. Hwang, Y.H. Song, J. Lim, Y.J. Ahn, Efficient white organic light emission by single emitting layer, Thin Solid Films 426 (2003) 246–249.
[7] J. Kido, K. Hongawa, K. Okuyama, K. Nagai, White light-emitting organic electroluminescent devices using the poly(N-vinylcarbazole) emitter layer doped with three fluorescent dyes, Appl. Phys. Lett. 64 (1994) 815–817.
[8] A.R. Duggal, J.J. Shiang, C.M. Heller, D.F. Foust, Organic light-emitting devices for illumination quality white light, Appl. Phys. Lett. 80 (2002) 3470–3472.
[9] Y. Shen, M.W. Klein, D.B. Jacobs, J. Scott Campbell, G.G. Malliaras, Mobility-dependent charge injection into an organic semiconductor, Phys. Rev. Lett. 86 (2001) 3867–3870.
[10] Y.B. Yuan, S. L, Z. W, H.T. X, X. Z, White organic light-emitting diodes combining vacuum deposited blue electrophosphorescent devices with red surface color conversion layers, Opt. Express 17 (2009) 1577–1582.
[11] G. Lei, L. Wang, Y. Qiu, Blue phosphorescent dye as sensitizer and emitter for white organic light-Emitting diodes, Appl. Phys. Lett. 85 (2004) 5403–5405.
[12] S. Tao, C.S. Lee, S.T. Lee, X. Zhang, Efficient blue and white organic light-emitting devices based on a single bipolar emitter, Appl. Phys. Lett. 91 (2007), 013507–013507-013503.
[13] R. Sebastian, L. Frank, S. Gregor, S. Nico, W. Karsten, L. BjoRn, L. Karl, White

organic light-emitting diodes with fluorescent tube efficiency, Nature 459 (2009) 234–238.
[14] H. Yu-Hsuan, H. Ding-Wei, C. Yung-Ting, Y. Ya-Han, C. Chih-Wei, T. Wei-Cheng, C. Chin-Ti, W. Pei-Kuen, Improve efficiency of white organic light-emitting diodes by using nanosphere arrays in color conversion layers, Opt. Express 20 (2012) 3005–3014.
[15] C.-H. Chang, Y.-J. Lo, J.-L. Huang, Y.-F. Huang, H.-Y. Hung, Y.-F. Jang, H.-H. Chang, Using an embedded nanocomposite layer to increase color-conversion efficiency of organic light-emitting diodes, Org. Electron. 15 (2014) 1906–1912.
[16] W. Zhang, Y. Chen, L. Gan, J. Qing, X. Zhou, Y. Huang, Y. Yang, Y. Zhang, J. Ou, X. Chen, M. Qiu Zhang, Localized surface plasmon resonance enhanced blue light-emission of polyfluorene copolymer, J. Phys. Chem. Solids 75 (2014) 1340–1346.
[17] E. Hutter, J.H. Fendler, Exploitation of localized surface plasmon resonance, Adv. Mater. 16 (2004) 1685–1706.
[18] D. Gúrard, J.Ú. Wenger, A. Devilez, Strong electromagnetic confinement near dielectric microspheres to enhance single-molecule fluorescence, Opt. Express 16 (2008) 15297.
[19] H. Huang, H. Hu, H. Wang, K. Geng, Enhanced light output of dipole source in gan-based nanorod light-emitting diodes by silver localized surface plasmon, J. Nanomater. 2014 (2014) 1–8.
[20] Y.Y. Kim, W.J. Hyun, K.H. Park, S.J. Ye, O.O. Park, Synthesis of poly(3,4-ethylenedioxythiophene): poly(styrene sulfonate)-capped silver nanoparticles and their application to blue polymer light-emitting diodes, Korean J. Chem. Eng. 32 (2015) 534–539.
[21] K.L. Kelly, E. Coronado, L.L. Zhao, G.C. Schatz, The optical properties of metal nanoparticles: the influence of size, shape, and dielectric environment, J. Phys. Chem. B. 34 (2002) 668–677.
[22] S. Pan, L.J. Rothberg, Enhancement of platinum octaethyl porphyrin phosphorescence near nanotextured silver surfaces, J. Am. Chem. Soc. 127 (2005) 6087–6094.
[23] J.-W. Park, M.H. Ullah, S.S. Park, C.-S. Ha, Organic electroluminescent devices using quantum-size silver nanoparticles, J. Mater. Sci. Mater. Electron. 18 (2007) 393–397.
[24] B. Wiley, T. Herricks, Y. Sun, Y. Xia, Polyol synthesis of silver nanoparticles:65 use of chloride and oxygen to promote the formation of single-crystal, truncated cubes and tetrahedrons, Nano Lett. 4 (2004) 1733–1739.
[25] B. Wiley, T. Herricks, Y. Sun, Y. Xia, Polyol synthesis of silver nanoparticles: use of chloride and oxygen to promote the formation of single-crystal, truncated cubes and tetrahedrons, Nano Lett. 4 (2004) 1733–1739.
[26] Z. Qiang, L. Weiyang, M. Christine, Z. Jie, C. Jingyi, W. Long-Ping, X. Younan, Seed-Mediated synthesis of ag nanocubes with controllable edge lengths in the range of 30–200 nm and comparison of their optical properties, J. Am. Chem. Soc. 132 (2010) 11372–11378.
[27] K. Subrata, M. Vivek, N. Sanjun, S.F. Ravi, Polyelectrolyte mediated scalable synthesis of highly stable silver nanocubes in less than a minute using microwave irradiation, Nanotechnology 19 (2008) 2222–2229.
[28] J.G. Smith, J.A. Faucheaux, P.K. Jain, Plasmon resonances for solar energy harvesting: a mechanistic outlook, Nano Today 10 (2015) 67–80.
[29] J.W. Shin, D.H. Cho, J. Moon, C.W. Joo, S.K. Park, J. Lee, J.H. Han, N.S. Cho, J. Hwang, W.H. Jin, Random nano-structures as light extraction functionals for organic light-emitting diode applications, Org. Electron. 15 (2014) 196–202.
[30] J.-W. Shin, D.-H. Cho, J. Moon, C.W. Joo, J. Lee, J.W. Huh, S.K. Park, J.-H. Han, N.S. Cho, J. Hwang, H.Y. Chu, J.-I. Lee, Random nanostructure scattering layer for suppression of microcavity effect and light extraction in OLEDs, Opt. Lett. 39 (2014) 3527.